

A general approach for identifying protein epitopes targeted by antibody repertoires using whole proteomes

Michael L. Paull^{1*}, Tim Johnston¹, Kelly N. Ibsen¹, Joel D. Bozekowski¹ and Patrick S. Daugherty^{1*}

¹Department of Chemical Engineering, University of California Santa Barbara CA, 93106, USA.

*Corresponding authors

Email: michael.paull444@gmail.com

Email: psdaug@gmail.com

19

20

21

22

23

24

25

26 **Abstract**

27

28 Antibodies are essential to functional immunity, yet the epitopes targeted by antibody
29 repertoires remain largely uncharacterized. To aid in characterization, we developed a
30 generalizable strategy to identify antibody-binding epitopes within individual proteins and entire
31 proteomes. Specifically, we selected antibody-binding peptides for 273 distinct sera out of a
32 random library and identified the peptides using next-generation sequencing. To identify
33 antibody-binding epitopes and the antigens from which these epitopes were derived, we tiled the
34 sequences of candidate antigens into short overlapping subsequences of length k (k -mers). We
35 used the enrichment over background of these k -mers in the antibody-binding peptide dataset to
36 identify antibody-binding epitopes. As a positive control, we used this approach, termed K-mer
37 Tiling of Protein Epitopes (K-TOPE), to identify epitopes targeted by monoclonal and polyclonal
38 antibodies of well-characterized specificity, accurately recovering their known epitopes. K-
39 TOPE characterized a commonly targeted antigen from *Rhinovirus A*, identifying three epitopes
40 recognized by antibodies present in 83% of sera ($n = 250$). An analysis of 2,908 proteins from
41 400 viral taxa that infect humans revealed seven enterovirus epitopes and five Epstein-Barr virus
42 epitopes recognized by >30% of specimens. Analysis of *Staphylococcus* and *Streptococcus*
43 proteomes similarly revealed six epitopes recognized by >40% of specimens. These common
44 viral and bacterial epitopes exhibited excellent agreement with previously mapped epitopes.
45 Additionally, we identified 30 HSV2-specific epitopes that were 100% specific against HSV1 in
46 novel and previously reported antigens. The K-TOPE approach thus provides a powerful new
47 tool to elucidate the organisms, antigens, and epitopes targeted by human antibody repertoires.

48

49

50 **Introduction**

51

52 Immunological memory allows for rapid antibody responses towards diverse antigens
53 long after initial exposure. For example, the adaptive immune response to many vaccinations is
54 often sustained throughout an individual's lifetime [1]. This immunological information is
55 archived within the genes encoding B-cell and T-cell receptors along with the corresponding
56 receptor structures, but has proven difficult to characterize in a comprehensive manner. The
57 ability to more fully interrogate immunological memory could reveal exposures to pathogens,
58 commensal organisms, and allergens. Such information has proven useful for correlating
59 antibody responses with disease outcomes to design more effective vaccines [2]. A detailed
60 record of immune exposures can also facilitate the identification of biomarkers to diagnose
61 infectious [3], autoimmune [4], and allergic conditions [5]. Furthermore, the capability to
62 broadly characterize antibody repertoires at the epitope level could be used to identify conserved
63 pathogen epitopes [6] and tumor specific antigen epitopes [7] to aid in therapeutic discovery.

64

65 A disease with prominent antibody responses is the common viral infection HSV, which
66 causes human infections in the orofacial region ("cold sores") and the genital region ("genital
67 ulcers") [8]. In 2012, the global prevalence of HSV1 was 3.7 billion people ages 0-49 [9] and the
68 global prevalence of HSV2 was 417 million people ages 15-49 [10]. Diagnostic discovery
69 generally focuses on diagnosing HSV2, since HSV2 infections can exacerbate HIV infections
70 [10]. However, HSV1 and HSV2 contain the same genes [11] and the protein-coding regions of
71 the HSV1 and HSV2 genomes share 83% sequence homology [12]. Therefore, researchers have
72 often analyzed HSV glycoprotein G, since it differs substantially between the two HSV species
73 [13]. In general, efforts have been limited to analyses of the surface-exposed envelope

73 glycoproteins [14–17], using approaches such as microarrays [18]. Therefore, it would be novel
74 to probe immunological memory using the entire proteomes of HSV1 and HSV2.

75 Immunological memory has been investigated extensively through sequencing the
76 variable regions of B- and T-cell receptor encoding genes amplified from circulating cells [19].

77 These methods have proven useful for identifying receptor-encoding genes that associate with
78 vaccination [20]. Nevertheless, such genetic information has not generally provided insight into
79 the specific environmental antigens and epitopes targeted, unless they are known *a priori*.

80 Furthermore, these methods require large specimen volumes (>10 mL) to obtain a sufficient
81 quantity of cells [20]. Thus, there remains a need for methods that identify the diverse antigen
82 targets of adaptive immunity.

83 Several methods have been developed to profile the protein epitopes of the secreted
84 antibody repertoire [21]. Approaches have often focused on linear epitopes since 85% of
85 epitopes contain at least one contiguous stretch of five amino acids [22]. By analyzing linear
86 epitopes, researchers have identified sensitive and specific diagnostic epitopes for numerous
87 diseases [21]. One common approach to epitope mapping is to generate short overlapping
88 peptides by tiling candidate antigens. These peptides are then assayed for serum antibody
89 reactivity in peptide microarray [23] or bacteriophage display library [24] formats. However,
90 because these methods are biased towards specific organisms, they do not enable comprehensive
91 or hypothesis-free immune evaluation. One strategy to overcome the limitations of tiling
92 experiments is to use fully random peptide libraries [5,25,26]. Here, experiments are less biased
93 and methods can analyze epitopes corresponding to a variety of organisms and antigens. A
94 disadvantage of microarrays is that they are typically several orders of magnitude less diverse
95 than peptide display libraries (e.g. 10^5 [25] versus 10^{10} [5]), limiting the effectiveness with which

96 current methods can achieve epitope discovery for low titer antibodies. In random library
97 experiments, epitopes are typically discovered using *de novo* motif discovery by unsupervised
98 clustering [27]. The most widely used algorithm for this purpose, MEME, scales approximately
99 quadratically with the number of input sequences, making it less useful for analyzing large
100 datasets resulting from next generation sequencing (NGS). While full-length antibody-binding
101 peptides can be analyzed, the majority of the binding energy is typically derived from just 5-6
102 amino acids [28], thus other amino acids within the peptide will contribute noise. To rectify this
103 problem researchers developed the IMUNE algorithm to reduce peptide datasets into statistically
104 enriched patterns and cluster these patterns to build motifs [29].

105 A significant challenge for epitope mapping approaches is the association of epitopes and
106 motifs with their corresponding antigens. Neither MEME nor IMUNE have the integrated
107 capability to connect motifs to plausible antigens. Also, motifs identified through these methods
108 often fail to reach the seven amino acids requirement for unambiguous identification of antigens
109 within the full database of protein sequences [30]. Fundamentally, linear stretches in epitopes are
110 typically less than seven amino acids in length [22], therefore, protein database searches of
111 individual epitopes (such as through BLAST [31]) often fail to achieve statistical significance.
112 Using multiple epitope matches within a single candidate antigen can increase the confidence of
113 antigen prediction [26,32]. However, this method is insufficient for antigens with a single
114 important epitope. Additionally, protein database searches are conducted using short amino acid
115 sequences, therefore these searches do not fully leverage large quantitative binding datasets. To
116 address these challenges, we present a general approach for associating epitopes with antigens
117 using large peptide datasets. The K-mer Tiling of Protein Epitopes (K-TOPE) algorithm
118 identifies epitopes by computationally tiling candidate antigens into k-mers, which are then

119 evaluated within large datasets of antibody-binding peptides. Here, we demonstrate the utility of
120 this approach by identifying linear epitopes within the proteomes of several prevalent infectious
121 pathogens.

122 **Results**

123

124 To enable the identification of protein epitopes bound by serum antibodies, we developed
125 a method that uses a database of antibody-binding peptides to identify epitopes in known protein
126 sequences (Fig 1). First, we selected peptides binding to an individual antibody repertoire within
127 a specimen (serum or plasma) from a bacterial display peptide library with 10^{10} random 12-mer
128 members. Then, we identified antibody-binding peptide sequences using NGS. To allow for the
129 manipulation of 20^5 (3.2 million) k-mers rather than full-length peptides, we processed peptides
130 into subsequences and evaluated the enrichments of all k-mers of length 5 [29]. Next, K-TOPE
131 tiled candidate antigen sequences, such as from a proteome, into overlapping k-mers. K-TOPE
132 used the enrichment values for these k-mers to construct an enrichment histogram across the
133 length of each protein sequence. The frequency value at each sequence position in the histogram
134 was proportional to the enrichment of k-mers that included that position. Specifically, for all k-
135 mers overlapping a position, we summed the log base 2 of the k-mer enrichment. Thus, higher
136 frequency values at a position in a protein sequence corresponded to a greater probability that a
137 position was included in an epitope. Epitopes were extracted from the maxima in the histogram
138 and scored based on their area under the curve (AUC). Finally, epitopes were assigned an
139 “epitope percentile” based on their rank in a list of scores generated from random proteins.

140 **Fig 1. K-TOPE determines epitopes by tiling proteins into k-mers.** (A) The input to the
141 algorithm is a dataset of approximately 10^6 peptides that were bound by serum antibodies. (B)
142 All 5-mers are evaluated for their enrichment in the list of peptides. (C) A portion of a protein
143 sequence is tiled into 5-mers which are weighted by their enrichment. This determines a
144 “frequency” value for each position in the sequence. (D) The frequency value for each position

145 in a protein sequence is plotted as a histogram. Possible epitopes are highlighted in pink on the
146 graph. Epitope sequences, area under the curve (AUC) scores, and significance percentiles are
147 displayed.

148

149 To assess the utility of K-TOPE, we first determined epitopes for monoclonal and
150 polyclonal antibodies that bind specific, well-defined epitopes in cMyc, V5, and amyloid beta.
151 We spiked these antibodies into serum at a final concentration of 25 nM and then selected and
152 identified binding peptides. K-TOPE identified epitopes that corresponded closely to the
153 previously reported epitopes of these antibodies (Fig 2). Importantly, the enrichment histograms
154 generated by antibodies spiked into background serum or buffer were nearly identical (S1 Fig),
155 suggesting that the noisy serum environment minimally affected epitope identification.

156 **Fig 2. K-TOPE found epitopes for antibodies with known specificity spiked into serum.**
157 Histograms for antibodies with known specificity against amyloid beta (P05067), cMyc
158 (P01106), and V5 (P11207) had prominent epitopes (in pink). (A) K-TOPE analysis of amyloid
159 beta determined the epitope VKM^{DAE}FRHD (668-678). This antibody was raised to whole
160 protein and is known from literature to have a conformation-specific discontinuous epitope that
161 maps to segments EFRHDSGY (673-680) and ED (692-693). (B) K-TOPE analysis of cMyc
162 determined the epitope EEQKL^{ISEED}LLRKR (408-422). This antibody was raised to
163 AEEQKL^{ISEED}LLRKRRE (407-424). (C) K-TOPE analysis of V5 determined the epitope
164 PIPNPLLGLDS (96-106). The antibody was raised to GKPIP^NPLLGLDST (94-107).
165

166

166 To identify “public epitopes” conserved across many individuals, epitopes were
167 generated for each specimen individually and then clustered. Although many private epitopes
168 were identified for each specimen in this process, we focused on the far smaller set of public
169 epitopes to facilitate comparison with previous literature. Given the ubiquity of exposure to the
170 upper respiratory pathogen *Rhinovirus A*, we validated the approach by identifying epitopes
171 within its genome polyprotein. Using a unique set of 250 serum specimens, we identified
172 epitopes within *Rhinovirus A* that were targeted by 30% or more of the specimens (Fig 3A). Of
173 the 250 specimens, 87% exhibited binding to at least one of these consensus epitopes (Fig 3B).
174 Three of these epitopes were located within positions 570-620 (Fig 3C), in the antigenic

175 attachment region of VP1. A fourth epitope within the VP2 region of the *Rhinovirus A* genome
176 polyprotein was targeted by 43% of the population.

177 **Fig 3. K-TOPE identified four epitopes in the *Rhinovirus A* genome polyprotein.** (A) K-
178 TOPE was applied to the *Rhinovirus A* genome polyprotein (P07210) for 250 specimens.
179 Histograms for all specimens are shown as rows in a heat map. The specimens have been
180 clustered such that specimens that bind the same epitopes are adjacent. Regions that contain
181 epitopes are outlined by dotted lines. (B) A table of the percentage of the population that bound
182 each epitope. For instance, Epitope 1 is the percentage of specimens that targeted “1”, “1+2”,
183 “1+3”, “1+4”, “1+2+3”, “1+2+4”, “1+2+3+4”. (C) The region from positions 570-620 is divided
184 into 3 sections that correspond to distinct epitopes. These epitopes are consensus epitopes which
185 were present in >30% of the 250 specimens. (D) Bar graph showing membership in different
186 epitope groups. For example, a specimen that binds epitopes 2 and 3 will belong to epitope group
187 “2+3”. In this population, 87% of the specimens bound at least one of the consensus epitopes.
188 The sequences of the epitopes were 1: QNPVENYI, 2: DSVLEVLLVVPN, 3:
189 APALDAAETGHT, and 4: NHTHPGEQG.
190

191 To assess trends in the population, each specimen was assigned into one of eight groups
192 based on which of the three VP1 epitopes were bound (Fig 3D). Notably, epitope binding was
193 not independent, since the group of specimens targeting all three epitopes was 44% larger than
194 expected and the group targeting epitopes ‘1+3’ was 50% smaller than expected (S1 Table). The
195 average age of the subset of specimens of known age (n=138) was 35 years, however, the epitope
196 group targeting all three epitopes had an average age of 17, and the epitope group targeting none
197 of the epitopes had an average age of 50 (S2 Table). Thus, people who targeted fewer *Rhinovirus*
198 *A* epitopes tended to be older.

199 Next, we investigated the utility of using K-TOPE to identify epitopes within a set of
200 2,908 proteins from 400 viral taxa with human tropism. This approach yielded 29 epitopes that
201 were bound by at least 30% of all specimens (Table 1). The prevalence of each epitope is noted,
202 which is defined as the proportion of specimens that bound the epitope. Some of these epitopes
203 have been reported previously [6,33–35]. Thus, a modest number of prominent linear viral
204 epitopes were bound by >30% of the specimens analyzed. A common antigen identified from

205 this analysis was Epstein-Barr nuclear antigen 1 (EBNA1) from Epstein-Barr virus (EBV),
206 which is expressed in EBV-infected cells [36]. Additionally, the epitopes identified for the
207 enterovirus genus were consistent with the epitopes identified for *Rhinovirus* A, which is a
208 species in that genus (Fig 3). Several of the epitopes were likely due to false discovery (e.g.,
209 Mayaro virus and Lyssavirus), since these viruses are uncommon in a general population. There
210 is an intrinsic lower limit on false positives since antibodies only bind 5-6 amino acids, which is
211 not enough information to uniquely specify a protein subsequence. This limitation is especially
212 pronounced among evolutionarily related proteins in closely related species.

213 **Table 1. A collection of 29 viral epitopes to which >30% of 250 specimens bound.**

Epitope	Protein	Taxon	Accession	Prevalence
DSVLNEVLVPN	Genome polyprotein	Enterovirus	P07210	0.668
PALTAETG	Genome polyprotein	Enterovirus	Q66575	0.588
GRRPFFHPV	Epstein-Barr nuclear antigen 1	Epstein-Barr virus (strain GD1)	Q1HVF7	0.524
AGAGGGAGA	Epstein-Barr nuclear antigen 1	Epstein-Barr virus (strain GD1)	Q1HVF7	0.516
KYTHPGEA	Genome polyprotein	Enterovirus	Q82122	0.492
VRRPFFSD	Protein UL84	Human cytomegalovirus	P16727	0.452
NPVERYVDE	Genome polyprotein	Enterovirus	Q82122	0.428
MVVPEFK	DNA-binding protein	Human mastadenovirus C	P03265	0.428
EVKLPHWTPT	Glycoprotein 42	Epstein-Barr virus (strain GD1)	P03205	0.42
KPQPEKPK	Structural polyprotein	Mayaro virus	Q8QZ72	0.416
GGAGAGGAGAGGG	Epstein-Barr nuclear antigen 1	Epstein-Barr virus (strain GD1)	P03211	0.412
ININRPLE	Large structural protein	Lyssavirus	Q9QSP0	0.412
RPSCIGCKG	Epstein-Barr nuclear antigen 1	Epstein-Barr virus (strain GD1)	P03211	0.404
GAGAGAGGG	Packaging protein UL32	Simplexvirus	P89455	0.376
LEEVIVEKTK	Genome polyprotein	Enterovirus	Q82081	0.352
KHTHPGI	Replication origin-binding protein	Human herpesvirus 3	P09299	0.352
AETGHTNKI	Genome polyprotein	Enterovirus	Q82122	0.344
YVFPHWITK	Envelope glycoprotein gp63	Primate T-lymphotropic virus 3	Q0R5Q9	0.34
KTNTTTNT	Immediate-early protein 2	Roseolovirus	Q9QJ16	0.34
MAADKPTL	Genome polyprotein	Murray Valley encephalitis virus	P05769	0.34
SFIVPEFA	Virion membrane protein A16	Orthopoxvirus	P16710	0.332
LVLPHWYMA	Cytoplasmic envelopment protein 1	Simplexvirus	P89430	0.328
YVDDMLNDI	Large tegument protein deneddylase	Human herpesvirus 6A (strain Uganda-1102)	P52340	0.328

SSGPKHTQKV	Genome polyprotein	Enterovirus	P03303	0.324
PVPEFQA	Non-structural polyprotein	Semliki forest virus	P08411	0.316
VPVTPNIAI	Genome polyprotein	Hepatitis C virus	Q68749	0.304
LHRPALT	Minor capsid protein L2	Human papillomavirus type 34	P36758	0.304
EHILNRPTG	RNA-directed RNA polymerase L	Crimean-Congo hemorrhagic fever orthonaivirus	Q6TQR6	0.304
GEFIGSE	Shutoff alkaline exonuclease	Human herpesvirus 8	Q2HR95	0.3

214 K-TOPE was used to analyze 2,908 proteins from viruses with human tropism. This search
215 demonstrated that only a few prominent linear viral epitopes were bound by a large portion of the
216 population.

217
218 We performed a similar analysis for the proteomes of the genera *Streptococcus* and
219 *Staphylococcus*, which are common bacterial human pathogens with 2,976 and 3,071 proteins in
220 their respective proteomes. K-TOPE was used with each of these proteomes to determine
221 epitopes bound by >30% of a population of 250 specimens, yielding 9 epitopes for *Streptococcus*
222 and 13 epitopes for *Staphylococcus* (Table 2). The epitope LIPEFIG(R) in ATP-dependent Clp
223 protease ATP-binding subunit ClpX was the most prevalent *Streptococcus* epitope and second
224 most prevalent *Staphylococcus* epitope. Therefore, K-TOPE could not determine which genus
225 generated this epitope. The most prevalent *Staphylococcus* epitope was PTHYVPEFKGS from
226 extracellular matrix protein-binding protein emp, which is a known virulence factor [37]. For
227 *Streptococcus*, the second most prevalent epitope was GQKMDDMLNS from the highly
228 antigenic Streptolysin O protein [38]. This epitope falls within a 70 amino acid range in
229 Streptolysin O that is known to bind antibodies [39]. The sequence “DKP” was present in 5/9
230 *Streptococcus* epitopes and the sequence “PEFXG” was present in 6/13 *Staphylococcus* epitopes
231 (Table 2). Therefore, there are multiple candidate antigens that may correspond to these highly
232 enriched sequences.

233

234 **Table 2. Epitopes in the proteomes of the genera *Staphylococcus* and *Streptococcus* which**

235 were bound by >30% of 250 specimens.

Epitope	Protein	Accession	Prevalence
<i>Streptococcus</i>			
LIPEFIGR	ATP-dependent Clp protease ATP-binding subunit ClpX	P63793	0.512
GQKMDDMLNS	Streptolysin O	Q5XE40	0.436
QIPALDKPL	FMN-dependent NADH-azoreductase	A4W2Z7	0.416
IADKPILD	UPF0154 protein SSU05_1707	A4VX34	0.392
TVADKPVA	Phenylalanine--tRNA ligase beta subunit	Q5XCX3	0.360
RTPDKPT	Agglutinin receptor	P16952	0.324
VVPNIWR	Putative 2-dehydropantoate 2-reductase	P65666	0.320
LLNRPIHD	CCA-adding enzyme	Q5M153	0.320
TLADKPEF	Autolysin	P06653	0.308
<i>Staphylococcus</i>			
PTHYVPEFKGS	Extracellular matrix protein-binding protein emp	Q2FIK4	0.572
LIPEFIG	ATP-dependent Clp protease ATP-binding subunit ClpX	B9DNC0	0.508
NKPEFSGAT	3-isopropylmalate dehydratase small subunit	Q4L7U3	0.436
NKNNKNNKN	Translation initiation factor IF-2	Q4L5X1	0.372
KLGNIVPEYK	Extracellular matrix protein-binding protein emp	P0C6P1	0.360
KLCRICFRE	30S ribosomal protein S14 type Z	Q5HM12	0.352
DFLNRPVD	Proline--tRNA ligase	Q4L5W5	0.348
EKNNNNNNNNNS	Alkaline shock protein 23	Q4L860	0.320
GVVPNISR	UvrABC system protein A	Q5HHQ9	0.312
LIPEFNQV	Homoserine kinase	Q8CSQ2	0.308
SPEFLGSQ	Undecaprenyl-diphosphatase	B9DK59	0.308
VGINRPTY	Putative glycosyltransferase TagX	O05154	0.308
VIPEFNND	Peptide chain release factor 2	Q4L4H9	0.300

236 K-TOPE was used to analyze 2,976 proteins from *Streptococcus* and 3,071 proteins from
237 *Staphylococcus*.

238
239 The most prevalent epitopes identified through proteome searches were validated by
240 comparison to previously reported epitopes. We chose to analyze the viral proteins EBNA1 from
241 EBV and the *Poliovirus 1* genome polyprotein (representing Enterovirus), which were present
242 five and seven times, respectively, in Table 1. Bacterial proteins chosen for validation were
243 Streptolysin O, corresponding to the second most prevalent *Streptococcus* epitope (Table 2), and
244 Extracellular matrix protein-binding protein emp, corresponding to most prevalent
245 *Staphylococcus* epitope (Table 2). In all cases, K-TOPE found prominent peaks in the histograms
246 that corresponded to reported epitopes (Fig 4) [6,33,35,40]. Additionally, K-TOPE identified an
247 immunogenic region of GA-repeats from positions 100-350 in the analysis of EBNA1 [23]. We

248 used a nonparametric statistical test to assign significance to the overlap between K-TOPE
249 epitopes and known epitopes. Using this method, all epitopes evaluated using K-TOPE had P-
250 values below 0.05 (Fig 4C).

251 **Fig 4. Epitopes identified through proteome searches were validated using literature-
252 reported epitopes.** In (A), (B), and (C), a histogram is shown for a single specimen with
253 significant peaks (in pink). To the right of the histogram is a heat map for 250 specimens. For
254 (A), there is a region of antigenic GA-repeats from positions 100-350. The table in (D) provides
255 the statistical significance of agreement between literature epitopes and K-TOPE epitopes for the
256 labeled peaks in (A), (B), and (C). The UniProt accessions used for this analysis were P03211 for
257 EBNA1, Q8NXI8 for extracellular matrix protein emp, and P03300 for
258 *Poliovirus 1* Genome Polyprotein. Statistical tests where epitopes with >50% GA content were
259 removed are denoted by an asterisk “*”. All identified epitopes had p-values below 0.05.
260

261 To identify HSV species-specific epitopes, we analyzed 12 HSV2 specimens and 10
262 HSV1 specimens. Since these viruses share many of the same proteins in their proteomes [11],
263 HSV1 specimens were appropriate controls for HSV2 specimens and vice-versa. To begin, we
264 identified species-specific epitopes in glycoprotein G, which is a protein that varies significantly
265 between the two species (Fig 5) [41]. There was a single HSV1 epitope, PMPSIGLEE, bound by
266 40% of HSV1 specimens and a single HSV2 epitope, GGPEEFEGAGD, bound by all HSV2
267 specimens. This HSV2-specific epitope aligned well with previous epitopes found for
268 glycoprotein G2 [13,42,43] (Table 3). Also, this epitope has been validated as an HSV2-specific
269 diagnostic [44,45]. The HSV1-specific epitope was also similar to the previously reported
270 epitope DHTPPMPSIGLE [18]. Interestingly, the two HSV-specific epitopes terminated in an
271 identical 7-mer sequence EGAGDGE (PMPSIGLEEEEEEGAGDGE and
272 GGPEEFEGAGDGE) [42]. This suggests that the regions containing these epitopes may be
273 evolutionarily or structurally related targets of the immune system.

274

275 **Table 3. Alignment of an HSV2-specific glycoprotein G2 epitope with previously reported**
276 **epitopes.**

Peptides														Reference
GG														K-TOPE
P														[13]
P														[42]
A														[43]

277

278 **Fig 5. K-TOPE identified epitopes for glycoprotein G1 using HSV1 specimens and for**
279 **glycoprotein G2 using HSV2 specimens.** For glycoprotein G1, a representative histogram for a
280 single specimen is shown in (A) and a heat map for all HSV1 specimens is shown in (C). For
281 glycoprotein G2, a representative histogram for a single specimen is shown in (B) and a heat
282 map for all HSV2 specimens is shown in (D). There was a single epitope identified for each
283 protein.

284

285 To identify candidate HSV species-specific epitopes, we analyzed the HSV1 and HSV2
286 proteomes. We identified 30 HSV2-specific epitopes that were 100% specific with prevalence >
287 30% (Table 4). Notably, 11 of these epitopes were bound by all HSV2 specimens. K-TOPE
288 identified a glycoprotein C epitope PRTTPTPPQ with 83% prevalence which was contained in a
289 previously identified epitope RN ASAPRTTPTPPQPRKATK [18]. In contrast to the numerous
290 HSV2-specific epitopes, only 4 HSV1-specific epitopes were identified, and the highest
291 prevalence achieved was only 40% (Table 5). One of these epitopes, RIRLPHI, overlapped with
292 the previously identified epitope HRRTRKAPKRIRLPHIR [46] in the well-described antigen
293 glycoprotein D [17]. One possible explanation for the discovery of fewer HSV1-specific epitopes
294 is that the HSV2 specimens had high IgM levels, whereas the HSV1 specimens had high IgG
295 levels. Since high IgM levels occur with severe recurrent herpes infections [47], we would
296 expect the high IgM HSV2 sera to yield more epitopes.

297

298

299

300 **Table 4. HSV2-specific epitopes were identified.**

Epitope	Protein	Accession	Prevalence
GGPEEFEGAGD	Envelope glycoprotein G	P13290	1
PLYARTTPAKF	Tegument protein UL47	P89467	1
VDSQRLTPGGSVS	Tegument protein UL21	P89444	1
KARKKGTTSAL	Envelope glycoprotein B	P08666	1
TPLRYACVL	Tegument protein UL47	P89467	1
ANSPWAPVL	mRNA export factor	P28276	1
RYSPHLN	Envelope glycoprotein B	P08666	1
EAMLNDAR	Large tegument protein deneddylase	P89459	1
QRLTPH	Large tegument protein deneddylase	P89459	1
LRYTPAGEV	Envelope glycoprotein H	P89445	1
RTPSMR	Major viral transcription factor ICP4 homolog	P90493	1
LATNNA	Small capsomere-interacting protein	P89458	0.917
LRTNNL	Ribonucleoside-diphosphate reductase small subunit	P69521	0.917
PRTTPTPPQ	Envelope glycoprotein C	Q89730	0.833
HRLYAVVA	Inner tegument protein	P89460	0.833
PSTPAMLNLG	Ribonucleoside-diphosphate reductase large subunit	P89462	0.667
VTKHTALCAR	Large tegument protein deneddylase	P89459	0.583
TRDYAGL	Envelope glycoprotein I	P13291	0.583
RLTVAQ	Envelope glycoprotein I	P13291	0.583
RSLGIA	Protein UL20	P89443	0.583
IRDLARTFA	Thymidine kinase	P89446	0.5
DITAKHRCL	Major capsid protein	P89442	0.5
ETPAQPPRY	Capsid scaffolding protein	P89449	0.5
VSGITPTQ	Tripartite terminase subunit 1	P89451	0.5
HEELYYGPVS	Tegument protein VP22	P89468	0.417
IQDLAYAIV	Ribonucleoside-diphosphate reductase large subunit	P89462	0.417
GPAQRHTY	DNA polymerase catalytic subunit	P89453	0.417
YFEEYAYS	Envelope glycoprotein B	P08666	0.417
LDDFDL	Tegument protein VP16	P68336	0.417
AA RLIDALYAEFLGG	Envelope glycoprotein H	P89445	0.333

301 A total of 30 epitopes were identified that were 100% specific against HSV1.

302 **Table 5. HSV1-specific epitopes were identified.**

Epitope	Protein	Accession	Prevalence
RIRLPHI	Envelope glycoprotein D	Q69091	0.4
PMPSIGLEE	Envelope glycoprotein G	P06484	0.4
CAAFVNDYSLV	Major capsid protein	P06491	0.3
EMADTFLDT	ICP47 protein	P03170	0.3

303 Only 4 epitopes were identified that were 100% specific against HSV2.

304 We sought to determine whether the HSV2-specific epitopes were contained in proteins
305 that differed between the HSV species [41]. We determined 8 HSV2-specific epitopes with
306 sequences that were contained in both HSV proteomes (S3 Table). Our analysis suggested that

307 these epitopes were only targeted by HSV2 specimens, despite their presence in the HSV1
308 proteome. Thus, even sequences that are conserved between species could serve as species-
309 specific targets.

310 Discussion

311

312 Here, we present a generalizable methodology for identifying epitopes within candidate
313 immunogenic proteins. By tiling proteins into k-mers and evaluating those k-mers in a database
314 of antibody-binding peptides, we determined epitopes for individuals and a population.
315 Importantly, we have demonstrated that K-TOPE can identify disease-specific epitopes and
316 antigens. One of the main features of this approach is that it combines k-mers to determine
317 composite epitopes that may not explicitly exist in the peptide dataset. Another important
318 element is using an antigen sequence to identify epitopes, thereby surmounting the 7 amino acid
319 requirement for successful antigen identification [30].

320 The K-TOPE approach to epitope mapping differs from reported methods in several
321 important ways. While proteome-derived peptide libraries have been used to identify disease-
322 specific epitopes [33,48], these methods lack the flexibility to examine multiple proteomes. For
323 instance, separate libraries would be required to analyze both HSV1 and HSV2. Even a library
324 that contains peptides spanning all viral proteomes cannot easily be extended to much larger
325 bacterial or parasitic proteomes [24]. A disadvantage of microarrays is that they have far lower
326 5-mer coverage (~27% [32]), than surface display (~100%) which could limit the application of
327 k-mer approaches. Other algorithms have been developed that identify binding motifs in peptide
328 datasets, but they lack the integrated capability to connect motifs to protein antigens [49,50].
329 Also, the direct method of aligning peptides to sequences becomes computationally infeasible
330 with a large number of peptides and candidate antigens [51].

331 The heterogeneity of experimental approaches complicates the validation of putative
332 epitopes and their associated antigens. The Immune Epitope Database (IEDB) has an all-
333 inclusive representation of information [52], which may not reflect important distinctions in
334 experimental platforms, specimens, and data analysis techniques. For instance, there are likely
335 numerous false positive epitopes for highly studied organisms and few identified epitopes for
336 poorly studied organisms. Also, there is a lack of quantitative data reported for epitopes [53],
337 such as the proportion of a given population that binds an epitope. To address this lack of
338 information, we first used K-TOPE to analyze specimens for responses to common pathogens in
339 a general population. This allows newly identified “public epitopes” to be benchmarked by
340 nearly any set of serum specimens. We required that a proportion of the population bind an
341 epitope to reduce false positives. Although analysis of the variation in private epitopes could be
342 valuable for understanding the variation in immune responses, it would complicate validation.
343 We determined public epitopes in *Rhinovirus A* and showed that people who targeted fewer
344 *Rhinovirus A* epitopes tended to be older, perhaps due to immunosenescence [54], reduced
345 pathogen exposure, or a lower incidence of rhinovirus infections [55]. With a diverse group of
346 specimens, it was possible to confirm that the RRPFF epitope in EBV’s protein EBNA1 is a very
347 commonly targeted epitope [33]. Since the specimens used to determine public epitopes were not
348 assayed for responses to pathogens, acute and chronic infections could not be readily
349 distinguished from prior infections. These public epitopes could be further validated using
350 specimens with acute infections or using longitudinal studies to determine if these epitopes
351 appear upon vaccination [56]. We did not find epitopes corresponding to measles or rubella
352 vaccination, which is consistent with a recent study that comprehensively identified viral
353 epitopes [57]. This implies that for these viruses, high titer antibodies targeting linear epitopes

354 may not be present. For HSV1 and HSV2, we determined whether an epitope was specific by
355 analyzing specimens infected by both virus species. Unexpectedly, we demonstrated that even
356 epitopes present in the conserved regions of both species' proteomes could be species-specific.
357 The difference in binding was likely due to differences in the structure and post-translational
358 modifications of the proteins. For the HSV analysis, we validated epitopes using previous
359 studies, however, it was difficult to know *a priori* whether a non-validated epitope was novel or
360 spurious. In general, since studies use different specimens, experiments, and computational
361 analyses, it is unlikely for the epitopes of two studies to completely coincide.

362 K-TOPE provides a new tool for identifying diagnostic biomarkers, vaccine components,
363 and candidate therapeutic targets. This approach could be used in the iterative process of
364 designing a vaccine, since it would be useful to know which epitopes are elicited in a population
365 by vaccination. Vaccine formulation could be altered to maximize the percentage of the
366 population that targets epitopes associated with a positive disease outcome [2]. K-TOPE could
367 also enable the development of diagnostics that assign disease based on the presence of epitopes.
368 Since this method only involves a single experimental screen, in principle multiple diseases
369 could be simultaneously diagnosed [58]. By searching for consensus epitopes in a disease group
370 that are absent in a control group, K-TOPE can discover disease-specific epitopes. For an
371 autoimmune disease, the entire human proteome could be analyzed to determine autoantigen
372 epitopes [33]. Similarly, using clinical histories of viral infection, K-TOPE can analyze the
373 proteomes of suspected pathogens to link epitopes to infections [24]. With specimens that have
374 HLA information, it could be possible to detect a correlation between HLA type and bound
375 epitopes [59]. This could have implications for how we determine genetic predisposition to
376 immunological disease.

377 There are important limitations to the conditions in which this approach could be
378 successful. First, this approach is currently limited to the identification of linear epitopes.
379 However, since 85% of epitopes have at least one linear stretch of five amino acids [22],
380 conformational epitopes with linear segments may be represented in the datasets. We chose to
381 focus on linear epitopes since methods that identify conformational epitopes often require 3D
382 protein structures, which are scarce relative to the number of protein sequences. This report
383 focuses on epitopes from common pathogens which are high-titer, but it could be difficult to
384 detect rare antibody epitopes. Methods that selectively deplete out high-titer antibodies could
385 prove effective for probing rare antibodies [60]. Another limitation is that protein sequences tend
386 to have a large degree of conservation and redundancy [61], as demonstrated by the false
387 positives found in the viral epitope search. Thus, even for analyses of non-immunogenic
388 proteomes, false positives will occur due to evolutionary or coincidental sequence overlap with
389 immunogenic proteomes. The issue of false positives can be partially allayed by deliberately
390 choosing the set of investigated proteins, such that all proteins are plausible candidate antigens.
391 Sequence conservation was demonstrated with the Enterovirus epitope PALTAVETGATNPL
392 [35], as well as with the *Human herpesvirus 6A* epitope YVDDMLNDI (Table 1) which shares
393 the k-mer “DDMLN” with the *Streptococcus* epitope GQKMDDMLNS (Table 2). Generally, if
394 an epitope sequence is present identically in multiple antigens, all candidate antigens should be
395 considered equally plausible without further biological, epidemiological, or experimental
396 information. It is important to note that one of the purposes of K-TOPE is to reduce thousands of
397 candidate proteins to a small set of proteins that can be experimentally validated.

398 In summary, the present approach enables the discovery of epitopes within the proteomes
399 of any organism whose sequence is deposited into the protein database. The challenge of

400 associating epitopes with antigens can be surmounted by transforming sets of antibody-binding
401 peptides to k-mers and tiling proteins of interest. Advancements upon this paradigm may enable
402 comprehensive immunological evaluations from serum and other biological tissues.

403 **Materials and methods**

404

405 **Strains and reagents**

406 *E. coli* strain MC1061 was used with surface display vector pB33eCPX for all library
407 screening experiments. Protein A/G magnetic beads were from Thermo Scientific Pierce.
408 Antibodies with known specificity included C3956 rabbit anti-c-Myc polyclonal antibody
409 (Sigma), anti-beta amyloid 1-42 antibody [mOC31] - conformation-specific (ab201059)
410 (Abcam), and rabbit V8137 Anti-V5 polyclonal antibody (Sigma). Antibodies were spiked into
411 healthy donor serum at a concentration of 25 nM. All sera (n=273) were obtained as deidentified
412 specimens from biobanks according to institutional guidelines, (Biosafety authorization numbers
413 #201417, #201713), and handled according to CDC-recommended BSL2 guidelines.

414 **Bacterial peptide display and sequencing**

415 The bacterial peptide display screening protocol was carried out as previously described
416 [29,62]. Briefly, an *E. coli* library displaying approximately 8 billion different 12-mer peptides
417 was combined with 1:100 diluted serum. We used magnetic selection with Protein A/G beads to
418 isolate bacterial cells with bound antibodies. Then, we confirmed that this isolated fraction of
419 bacteria bound antibodies using flow cytometry. Amplicons were prepared from the isolated
420 fraction for sequencing using the Illumina NextSeq.

421 **Protein databases**

422 Protein sequences were obtained from UniProt or by using the Biopython module [63].
423 Accessions for proteins are noted in figures and figure captions. For the epitope validation,
424 accessions were chosen that reference the most highly annotated version of the proteins
425 identified in Table 1 and Table 2. The list of random proteins used for statistical analysis was
426 obtained through a UniProt search of “reviewed:yes”. The viral proteome search used a Uniref
427 search of “uniprot:(host:”homo sapiens” reviewed:yes fragment:no) AND identity:0.9” and
428 yielded 2,908 proteins. The *Staphylococcus* proteome search used a Uniref search of
429 “uniprot:(taxonomy:”Staphylococcus [1279]” fragment:no reviewed:yes) AND identity:0.9” and
430 yielded 3,071 proteins. The *Streptococcus* proteome search used a Uniref search of
431 “uniprot:(taxonomy:”Streptococcus [1301]” fragment:no reviewed:yes) AND identity:0.9” and
432 yielded 2,976 proteins. HSV analysis used a UniProt search of “reviewed:yes AND
433 organism:”Human herpesvirus 1 (strain 17) (HHV-1) (Human herpes simplex virus 1) [10299]”
434 AND proteome:up000009294” for HSV1, yielding 73 proteins and a Uniprot search of
435 “reviewed:yes AND organism:”Human herpesvirus 2 (strain HG52) (HHV-2) (Human herpes
436 simplex virus 2) [10315]” AND proteome:up000001874” for HSV2, yielding 72 proteins.

437 **Selection of literature epitopes**

438 For EBNA1, RRPFF was chosen because it was noted that RRPFF antibodies were found
439 in the serum of healthy individuals [33]. KRPSCIGCK was noted as an EBNA1 epitope that was
440 preferentially targeted by pre-eclamptic women, but was also targeted by healthy controls [6].
441 The motif XPEFXGSXX was discovered and inferred to correspond to VPEFKGSLP in
442 *Staphylococcus aureus* using protein database searches [40]. For *Poliovirus 1*, the epitope
443 PALTAVETGATNPL was found to be a cross-reactive epitope in many enteroviruses [35].

444 Sequence processing

445 All software files are posted on GitHub (<https://github.com/mlpaul/KTOPE>) and all 278
446 antibody-binding peptide files are available on Dryad (doi:10.5061/dryad.v7d0350). The imune-
447 processor.jar file is available for research, non-profit, and non-commercial use and requires a
448 license for commercial use. All other software is available under the MIT license. The algorithms
449 for generating nonredundant sequence lists from FASTQ files, outputting enrichment values for
450 subsequences, and exhaustively calculating k-mer statistics were adapted from IMUNE (imune-
451 processor.jar and calculate-patterns.jar) [29]. We added the capability to start with lists of
452 peptides rather than NGS data. The enrichment of a k-mer is defined as the ratio of the number
453 of observations of the k-mer to the “expected” number of observations. The “expected” value is
454 calculated as the product of the total number of sequences, the number of frames the k-mer could
455 fit in the sequences, and the probability of the k-mer appearing based on amino acid usage. If a
456 k-mer’s enrichment is above the “enrichment minimum” (2.0 for this study), it is used in K-
457 TOPE. K-mers need to be calculated only once per specimen. All interaction with IMUNE-
458 derived code is through a Python module which sets up a folder hierarchy and acts as a wrapper
459 for IMUNE-derived code (imuneprocessor.py). These programs are memory and hard-drive
460 intensive and it is recommended to have at least 16 GB of free RAM and 100 GB of hard-drive
461 space. Analysis was carried out on a Dell Optiplex 9020 with an Intel® Core™ i7-4790 CPU @
462 3.60 GHz, 64-bit operating system, and 32.0 GB of RAM. Processing FASTQ files into
463 subsequences from 12 specimens, each containing approximately 1.5 million unique sequences,
464 required 2.3 hours and calculating k-mer enrichment required 7.7 minutes. The duration of these
465 calculations scales approximately linearly with the number of specimens and sequences.

466 K-TOPE algorithm

467 The K-TOPE algorithm (Code S1) is written in Python 3.6 (KTOPE.py). A usage guide
468 for KTOPE is available (Text S1). First, there is a RAM-intensive step of loading k-mer
469 enrichment data into memory as a dictionary. The enrichment dictionary for 250 specimens
470 required approximately 4 GB of RAM. Then, a protein of interest is chosen for analysis and its
471 sequence is loaded. This protein is tiled into k-mers of a set length. For this study, 5-mers were
472 used. Each position in the protein sequence is assigned a frequency counter that starts at 0. The
473 frequency counter of each sequence position contained in an enriched k-mer is incremented by
474 the logarithm base 2 of the k-mer's enrichment. For instance, if 3 k-mers that overlapped at a
475 position had enrichments of 2, 4, and 8, the frequency for that position would be $\log_2 2 + \log_2 4$
476 $+ \log_2 8 = 6$. The frequency counters are compiled into a histogram which is smoothed using a
477 moving window. For this analysis, the window had width 7 and used linear weighting with 1 in
478 the center and 0.1 at the edges. Minima and maxima are identified in the smoothed histogram.
479 All intervals between 2 minima that contain a maximum are used to define epitopes. Epitopes
480 were limited to a minimum length of 6 and a maximum length of 15. Epitopes are scored using
481 the area under the curve of the un-smoothed histogram. To assign statistical significance to each
482 epitope, the epitope's score is ranked in a list of scores for epitopes of the same length generated
483 through an analysis of 10,000 random proteins. This rank is reported as a percentile in the
484 distribution of random protein epitope scores. For this study, a percentile cutoff of 95% was
485 used. For 12 specimens, analysis of 10,000 random proteins required 10.0 minutes.

486 After determining epitopes for individual specimens, K-TOPE can determine consensus
487 epitopes for a population. Each epitope is characterized by a “centroid” which is the weighted
488 central position of the epitope, indexed as a position in the protein sequence. Centroids for all

489 epitopes that meet the percentile cutoff are compiled. They are then clustered using k-means to
490 associate close centroids with the KMeans function from scikit-learn [64]. A representative
491 epitope is made for each cluster and kept if it meets a minimum prevalence in the population.
492 Closely overlapping epitopes are removed and the final list is sorted by prevalence. Consensus
493 epitopes can be determined for each protein in a proteome, generating a list of epitopes prevalent
494 in a population. Determination of consensus epitopes for the *Rhinovirus A* genome polyprotein
495 (P07210) for 250 specimens required 24.4 seconds. The proteome searches for viruses with
496 human tropism, *Staphylococcus*, and *Streptococcus* for 250 specimens required 3.1, 2.3, and 1.9
497 hours, respectively.

498 We calculated expected membership of epitope groups by multiplying the proportions of
499 the population that bound each epitope. For example, if epitope 1 was bound by 32% of the
500 population and epitope 2 was bound by 67%, then the expected membership of epitope group
501 ‘1+2’ would be 21%. We ranked the overlaps between K-TOPE derived epitopes and literature
502 epitopes in a list of 10,000 randomly generated epitope overlaps to determine a p-value. To
503 remove redundant epitopes found in the proteome searches, we used the PAM30 similarity
504 matrix to align two epitopes and compare each position to calculate a similarity score. Epitopes
505 that had similarity scores >10 , were in the same protein, and were from different organisms were
506 considered redundant. We removed the less prevalent of the two redundant epitopes.

507 The HSV analysis used “disease” group specimens to identify epitopes and “control”
508 group specimens to subtract epitopes. Epitopes were identified in the disease group that met the
509 epitope percentile cutoff (95%) and the minimum prevalence (30%). Then, all disease epitopes
510 were evaluated in the control group. For an epitope to be considered disease-specific, its score
511 had to be below the epitope percentile cutoff (80%) in all control specimens. To identify HSV2-

512 specific epitopes that were also in the HSV1 proteome, we identified epitopes that exactly
513 matched a subsequence in an HSV1 protein.

514 **Data visualization**

515 Fig 1 was created using Inkscape. Histograms and heat maps were generated using the
516 Matplotlib python module [65]. Bar graphs were generated using GraphPad Prism 7.

517

518 **Acknowledgements**

519

520 The authors acknowledge the use of the Biological Nanostructures Laboratory within the
521 California NanoSystems Institute, supported by the University of California, Santa Barbara and
522 the University of California, Office of the President. We would like to acknowledge the work of
523 Jack Reifert, Robert Pantazes, Chia-In Lin, Serra Elliott, and Kiho Song. We would like to
524 acknowledge Linc Johnson for help with the initial conceptualization of this project.

525

526

527

528

529

530

531

532

533

534

535

536

537 **References**

538

- 539 1. Amanna IJ, Carlson NE, Slifka MK. Duration of humoral immunity to common viral and
540 vaccine antigens. *N Engl J Med.* 2007;357: 1903–1915. doi:10.1542/peds.2008-
541 2139LLL
- 542 2. Soria-Guerra RE, Nieto-Gomez R, Govea-Alonso DO, Rosales-Mendoza S. An overview
543 of bioinformatics tools for epitope prediction: Implications on vaccine development. *J*
544 *Biomed Inform.* Elsevier Inc.; 2015;53: 405–414. doi:10.1016/j.jbi.2014.11.003
- 545 3. Lemon SM, Gates NL, Simms TE, Bancroft WH. IgM antibody to hepatitis B core antigen
546 as a diagnostic parameter of acute infection with hepatitis B virus. *J Infect Dis.* 1981;143:
547 803–809. doi:10.1093/infdis/143.6.803
- 548 4. Schellekens GA, Visser H, De Jong BA, Van Den Hoogen FH, Hazes JM, Breedveld FC,
549 et al. The diagnostic properties of rheumatoid arthritis antibodies recognizing a cyclic
550 citrullinated peptide. *Arthritis Rheum.* 2000;43: 155–163. doi:10.1002/1529-
551 0131(200001)43:1<155::AID-ANR20>3.0.CO;2-3
- 552 5. Spatola BN, Murray JA, Kagnoff M, Kaukinen K, Daugherty PS. Antibody repertoire
553 profiling using bacterial display identifies reactivity signatures of celiac disease. *Anal*
554 *Chem.* 2012;85: 1215–1222. doi:10.1021/ac303201d
- 555 6. Elliott SE, Parchim NF, Kellems RE, Xia Y, Soffici AR, Daugherty PS. A pre-eclampsia-
556 associated Epstein-Barr virus antibody cross-reacts with placental GPR50. *Clin Immunol.*
557 2016;168: 64–71. doi:10.1016/j.clim.2016.05.002
- 558 7. Gubin MM, Zhang X, Schuster H, Caron E, Ward JP, Noguchi T, et al. Checkpoint
559 blockade cancer immunotherapy targets tumour-specific mutant antigens. *Nature.*
560 2014;515: 577–581. doi:10.1038/nature13988
- 561 8. Taylor TJ, Brockman MA, McNamee EE, Knipe DM. Herpes simplex virus. *Front Biosci.*
562 2002;7: 752–764. doi:10.2741/taylor
- 563 9. Looker KJ, Magaret AS, May MT, Turner KME, Vickerman P, Gottlieb SL, et al. Global
564 and regional estimates of prevalent and incident herpes simplex virus type 1 infections in
565 2012. *PLoS One.* 2015;10: 1–17. doi:10.1371/journal.pone.0140765
- 566 10. Looker KJ, Magaret AS, Turner KME, Vickerman P, Gottlieb SL, Newman LM. Global
567 estimates of prevalent and incident herpes simplex virus type 2 infections in 2012. *PLoS*
568 *One.* 2015;10: 1–23. doi:10.1371/journal.pone.0114989
- 569 11. Bowden RJ, McGeoch DJ. Evolution of herpes simplex viruses. *Herpes simplex viruses.*
570 CRC Press; 2017.
- 571 12. Gupta R, Warren T, Wald A. Genital herpes. *Lancet.* 2007;370: 2127–2137.
572 doi:10.1016/S0140-6736(07)61908-4
- 573 13. Marsden HS, MacAulay K, Murray J, Smith IW. Identification of an immunodominant
574 sequential epitope in glycoprotein G of herpes simplex virus type 2 that is useful for

575 serotype-specific diagnosis. *J Med Virol.* 1998;56: 79–84. doi:10.1002/(SICI)1096-
576 9071(199809)56:1<79::AID-JMV13>3.0.CO;2-R

577 14. Clo E, Kracun SK, Nudelman AS, Jensen KJ, Liljeqvist J-A, Olofsson S, et al.
578 Characterization of the viral O-glycopeptidome: A novel tool of relevance for vaccine
579 design and serodiagnosis. *J Virol.* 2012;86: 6268–6278. doi:10.1128/JVI.00392-12

580 15. Pan M, Wang X, Liao J, Yin D, Li S, Pan Y, et al. Prediction and identification of
581 potential immunodominant epitopes in glycoproteins B, C, E, G, and i of herpes simplex
582 virus type 2. *Clin Dev Immunol.* 2012;2012. doi:10.1155/2012/205313

583 16. Liu K, Jiang D, Zhang L, Yao Z, Chen Z, Yu S, et al. Identification of B- and T-cell
584 epitopes from glycoprotein B of herpes simplex virus 2 and evaluation of their
585 immunogenicity and protection efficacy. *Vaccine.* Elsevier Ltd; 2012;30: 3034–3041.
586 doi:10.1016/j.vaccine.2011.10.010

587 17. Whitbeck JC, Huang Z-Y, Cairns TM, Gallagher JR, Lou H, Ponce-de-Leon M, et al.
588 Repertoire of epitopes recognized by serum IgG from humans vaccinated with herpes
589 simplex virus 2 glycoprotein D. *J Virol.* 2014;88: 7786–7795. doi:10.1128/JVI.00544-14

590 18. Risinger C, Sørensen KK, Jensen KJ, Olofsson S, Bergström T, Blixt O. Linear
591 multiepitope (glyco)peptides for type-specific serology of herpes simplex virus (HSV)
592 infections. *ACS Infect Dis.* 2017;3: 360–367. doi:10.1021/acsinfecdis.7b00001

593 19. Georgiou G, Ippolito GC, Beausang J, Busse CE, Wardemann H, Quake SR. The promise
594 and challenge of high-throughput sequencing of the antibody repertoire. *Nat Biotechnol.*
595 Nature Publishing Group; 2014;32: 158–68. doi:10.1038/nbt.2782

596 20. Lee J, Boutz DR, Chromikova V, Joyce MG, Vollmers C, Leung K, et al. Molecular-level
597 analysis of the serum antibody repertoire in young adults before and after seasonal
598 influenza vaccination. *Nat Med.* 2016;22: 1456–1464. doi:10.1038/nm.4224

599 21. Paull ML, Daugherty PS. Mapping serum antibody repertoires using peptide libraries.
600 *Curr Opin Chem Eng.* Elsevier Ltd; 2018;19: 21–26. doi:10.1016/j.coche.2017.12.001

601 22. Kringelum JV, Nielsen M, Padkjær SB, Lund O. Structural analysis of B-cell epitopes in
602 antibody:protein complexes. *Mol Immunol.* Elsevier Ltd; 2013;53: 24–34.
603 doi:10.1016/j.molimm.2012.06.001

604 23. Hecker M, Fitzner B, Wendt M, Lorenz P, Flechtner K, Steinbeck F, et al. High-density
605 peptide microarray analysis of IgG autoantibody reactivities in serum and cerebrospinal
606 fluid of multiple sclerosis patients. *Mol Cell Proteomics.* 2016;15: 1360–80.
607 doi:10.1074/mcp.M115.051664

608 24. Xu GJ, Kula T, Xu Q, Li MZ, Vernon SD, Ndung'u T, et al. Comprehensive serological
609 profiling of human populations using a synthetic human virome. *Science (80-).* 2015;348:
610 aaa0698. doi:10.1126/science.aaa0698

611 25. Legutki JB, Zhao Z-G, Greving M, Woodbury N, Johnston SA, Stafford P. Scalable high-
612 density peptide arrays for comprehensive health monitoring. *Nat Commun.* Nature
613 Publishing Group; 2014;5: 4785. doi:10.1038/ncomms5785

614 26. Liu X, Hu Q, Liu S, Tallo LJ, Sadzewicz L, Schettine CA, et al. Serum antibody repertoire
615 profiling using in silico antigen screen. *PLoS One*. 2013;8: e67181.
616 doi:10.1371/journal.pone.0067181

617 27. Bailey T, Elkan C. Unsupervised learning of multiple motifs using expected minimization.
618 *Mach Learn*. 1995;21: 51–80. doi:10.1007/BF00993379

619 28. Sykes KF, Legutki JB, Stafford P. Immunosignaturing: A critical review. *Trends*
620 *Biotechnol*. 2013;31: 45–51. doi:10.1016/j.tibtech.2012.10.012

621 29. Pantazes RJ, Reifert J, Bozekowski J, Ibsen KN, Murray JA, Daugherty PS. Identification
622 of disease-specific motifs in the antibody specificity repertoire via next-generation
623 sequencing. *Sci Rep*. 2016;6: 30312. doi:10.1038/srep30312

624 30. Bastas G, Sompuram SR, Pierce B, Vani K, Bogen SA. Bioinformatic requirements for
625 protein database searching using predicted epitopes from disease-associated antibodies.
626 *Mol Cell Proteomics*. 2007;7: 247–256. doi:10.1074/mcp.M700107-MCP200

627 31. Altschul SF, Gish W, Miller W, Myers EW, Lipman DJ. Basic local alignment search
628 tool. *J Mol Biol*. 1990;215: 403–10. doi:10.1016/S0022-2836(05)80360-2

629 32. Richer J, Johnston SA, Stafford P. Epitope identification from fixed-complexity random-
630 sequence peptide microarrays. *Mol Cell Proteomics*. 2015;14: 136–147.
631 doi:10.1074/mcp.M114.043513

632 33. Larman HB, Laserson U, Querol L, Verhaeghen K, Solimini NL, Xu GJ, et al. PhIP-Seq
633 characterization of autoantibodies from patients with multiple sclerosis, type 1 diabetes
634 and rheumatoid arthritis. *J Autoimmun*. 2013;43: 1–9. doi:10.1016/j.jaut.2013.01.013

635 34. Sundström P, Nyström M, Ruuth K, Lundgren E. Antibodies to specific EBNA-1 domains
636 and HLA DRB1*1501 interact as risk factors for multiple sclerosis. *J Neuroimmunol*.
637 Elsevier B.V.; 2009;215: 102–107. doi:10.1016/j.jneuroim.2009.08.004

638 35. Samuelson A, Forsgren M, Johansson BO, Wahren B. Molecular basis for serological
639 cross-reactivity between enteroviruses. *Clin Diagn Lab Immunol*. 1994;1: 336–341.

640 36. Young LS, Rickinson AB. Epstein-Barr virus: 40 years on. *Nat Rev Cancer*. 2004;4: 757–
641 768. doi:10.1038/nrc1452

642 37. Romero Pastrana F, Neef J, Koedijk DGAM, de Graaf D, Duipmans J, Jonkman MF, et al.
643 Human antibody responses against non-covalently cell wall-bound *Staphylococcus aureus*
644 proteins. *Sci Rep*. 2018;8: 3234. doi:10.1038/s41598-018-21724-z

645 38. Kaplan EL, Huwe BB. The sensitivity and specificity of an agglutination test for
646 antibodies to streptococcal extracellular antigens: A quantitative analysis and comparison
647 of the streptozyme test with the anti-streptolysin O and anti-deoxyribonuclease B tests. *J*
648 *Pediatr*. 1980;96: 367–373. doi:10.1016/S0022-3476(80)80674-3

649 39. Mortensen R, Nissen TN, Fredslund S, Rosenkrands I, Christensen JP, Andersen P, et al.
650 Identifying protective *Streptococcus pyogenes* vaccine antigens recognized by both B and
651 T cells in human adults and children. *Sci Rep*. Nature Publishing Group; 2016;6: 22030.
652 doi:10.1038/srep22030

653 40. Weber LK, Palermo A, Kügler J, Armant O, Isse A, Rentschler S, et al. Single amino acid
654 fingerprinting of the human antibody repertoire with high density peptide arrays. *J
655 Immunol Methods*. Elsevier B.V; 2017;443: 45–54. doi:10.1016/j.jim.2017.01.012

656 41. McGeoch DJ, Moss HWM, McNab D, Frame MC. DNA sequence and genetic content of
657 the HindIII 1 region in the short unique component of the herpes simplex virus type 2
658 genome: Identification of the gene encoding glycoprotein G, and evolutionary
659 comparisons. *J Gen Virol*. 1987;68: 19–38. doi:10.1099/0022-1317-68-1-19

660 42. Liljeqvist JA, Trybala E, Svennerholm B, Jeansson S, Sjögren-Jansson E, Bergström T.
661 Localization of type-specific epitopes of herpes simplex virus type 2 glycoprotein G
662 recognized by human and mouse antibodies. *J Gen Virol*. 1998;79: 1215–1224.
663 doi:10.1099/0022-1317-79-5-1215

664 43. Grabowska A, Jameson C, Laing P, Jeansson S, Sjögren-Jansson E, Taylor J, et al.
665 Identification of type-specific domains within glycoprotein G of herpes simplex virus type
666 2 (HSV-2) recognized by the majority of patients infected with HSV-2, but not by those
667 infected with HSV-1. *J Gen Virol*. 1999;80: 1789–1798. doi:10.1099/0022-1317-80-7-
668 1789

669 44. Oladepo DK, Klapper PE, Marsden HS. Peptide based enzyme-linked immunoassays for
670 detection of anti-HSV-2 IgG in human sera. *J Virol Methods*. 2000;87: 63–70.
671 doi:10.1016/S0166-0934(00)00152-X

672 45. Nilsen A, Ulvestad E, Marsden H, Langeland N, Myrmel H, Matre R, et al. Performance
673 characteristics of a glycoprotein G based oligopeptide (peptide 55) and two different
674 methods using the complete glycoprotein as assays for detection of anti-HSV-2 antibodies
675 in human sera. *J Virol Methods*. 2003;107: 21–27. doi:10.1016/S0166-0934(02)00185-4

676 46. Eisenberg RJ, Long D, Ponce de Leon M, Matthews JT, Spear PG, Gibson MG, et al.
677 Localization of epitopes of herpes simplex virus type 1 glycoprotein D. *J Virol*. 1985;53:
678 634–644. Available:
679 http://www.ncbi.nlm.nih.gov/entrez/query.fcgi?cmd=Retrieve&db=PubMed&dopt=Citation&list_uids=2578577

681 47. Kalimo KO, Marttila RJ, Granfors K, Viljanen MK. Solid-phase radioimmunoassay of
682 human immunoglobulin M and immunoglobulin G antibodies against herpes simplex virus
683 type 1 capsid, envelope, and excreted antigens. *Infect Immun*. 1977;15: 883–9.

684 48. Carmona SJ, Nielsen M, Schafer-Nielsen C, Mucci J, Altcheh J, Balouz V, et al. Towards
685 high-throughput immunomics for infectious diseases: Use of next-generation peptide
686 microarrays for rapid discovery and mapping of antigenic determinants. *Mol Cell
687 Proteomics*. 2015;14: 1871–1884. doi:10.1074/mcp.M114.045906

688 49. Kim T, Tyndel MS, Huang H, Sidhu SS, Bader GD, Gfeller D, et al. MUSI: An integrated
689 system for identifying multiple specificity from very large peptide or nucleic acid data
690 sets. *Nucleic Acids Res*. 2012;40: e47. doi:10.1093/nar/gkr1294

691 50. Liu H, Han F, Zhou H, Yan X, Kosik KS. Fast motif discovery in short sequences. 2016
692 IEEE 32nd Int Conf Data Eng ICDE 2016. 2016;2016: 1158–1169.
693 doi:10.1109/ICDE.2016.7498321

694 51. Halperin RF, Stafford P, Emery JS, Navalkar K, Johnston SA. GuiTope: An application
695 for mapping random-sequence peptides to protein sequences. *BMC Bioinformatics*.
696 BioMed Central Ltd; 2012;13: 1. doi:10.1186/1471-2105-13-1

697 52. Peters B, Sidney J, Bourne P, Bui HH, Buus S, Doh G, et al. The immune epitope
698 database and analysis resource: From vision to blueprint. *PLoS Biol*. 2005;3: 0379–0381.
699 doi:10.1371/journal.pbio.0030091

700 53. Caoili SEC. Benchmarking B-cell epitope prediction with quantitative dose-response data
701 on antipeptide antibodies: Towards novel pharmaceutical product development. *Biomed
702 Res Int*. 2014;2014. doi:10.1155/2014/867905

703 54. Alter-Wolf S, Blomberg BB, Riley RL. Deviation of the B cell pathway in senescent mice
704 is associated with reduced surrogate light chain expression and altered immature B cell
705 generation, phenotype, and light chain expression. *J Immunol*. 2009;182: 138–47.
706 doi:10.1016/j.bbi.2008.05.010

707 55. Heikkinen T, Järvinen A. The common cold. *Lancet*. 2003;361: 51–59.
708 doi:10.1016/S0140-6736(03)12162-9

709 56. Stafford P, Wrapp D, Johnston SA. General assessment of humoral activity in healthy
710 humans. *Mol Cell Proteomics*. 2016;15: 1610–1621. doi:10.1074/mcp.M115.054601

711 57. Burnham CAD, McAdam AJ. Your viral past: A comprehensive method for serological
712 profiling to explore the human virome. *Clin Chem*. 2016;62: 426–427.
713 doi:10.1373/clinchem.2015.245027

714 58. Stafford P, Cichacz Z, Woodbury NW, Johnston SA. Immunosignature system for
715 diagnosis of cancer. *Proc Natl Acad Sci*. 2014;111: E3072–E3080.
716 doi:10.1073/pnas.1409432111

717 59. Palermo A, Weber LK, Rentschler S, Isse A, Sedlmayr M, Herbster K, et al. Identification
718 of a tetanus toxin specific epitope in single amino acid resolution. *Biotechnol J*.
719 2017;1700197: 1700197. doi:10.1002/biot.201700197

720 60. Bozekowski JD, Graham AJ, Daugherty PS. High-titer antibody depletion enhances
721 discovery of diverse serum antibody specificities. *J Immunol Methods*. Elsevier;
722 2018;455: 1–9. doi:10.1016/j.jim.2018.01.003

723 61. Suzek BE, Huang H, McGarvey P, Mazumder R, Wu CH. UniRef: Comprehensive and
724 non-redundant UniProt reference clusters. *Bioinformatics*. 2007;23: 1282–1288.
725 doi:10.1093/bioinformatics/btm098

726 62. Ibsen KN, Daugherty PS. Prediction of antibody structural epitopes via random peptide
727 library screening and next generation sequencing. *J Immunol Methods*. Elsevier;
728 2017;451: 28–36. doi:10.1016/j.jim.2017.08.004

729 63. Cock PJA, Antao T, Chang JT, Chapman BA, Cox CJ, Dalke A, et al. Biopython: Freely
730 available Python tools for computational molecular biology and bioinformatics.
731 *Bioinformatics*. 2009;25: 1422–1423. doi:10.1093/bioinformatics/btp163

732 64. Pedregosa F, Varoquaux G, Gramfort A, Michel V, Thirion B, Grisel O, et al. Scikit-learn:

733 Machine learning in Python. *J Mach Learn Res.* 2012;12: 2825–2830.
734 doi:10.1007/s13398-014-0173-7.2

735 65. Hunter JD. Matplotlib: A 2D graphics environment. *Comput Sci Eng.* 2007;9: 99–104.
736 doi:10.1109/MCSE.2007.55

737

738 **Supporting information**

739

740 **S1 Fig. A comparison of histograms generated by K-TOPE when antibodies were added to**
741 **serum or buffer.** Histograms were generated for antibodies against cMyc (P01106), V5
742 (P11207), and amyloid beta (P05067). The most prominent peaks were present regardless of
743 whether antibodies were added to serum or buffer. This suggests that the binding signature of a
744 single antibody was not obscured by the many other antibody specificities present in serum.

745

746 **S1 Table. The expected and actual membership of different epitope groups.** The expected
747 membership of epitope groups was calculated by multiplying the proportions of the population
748 that bound each epitope. For example, if epitope 1 was bound by 32% of the population and
749 epitope 2 was bound by 67%, then the expected membership of epitope group ‘1+2’ would be
750 21%. Note that specimens in groups *only* bound the epitopes in the groups e.g. specimens in
751 group ‘1’ did not bind ‘2’ or ‘3’. Generally, the actual and expected membership values agreed
752 except for the ‘1+2+3’ group which had higher membership than expected and the ‘1+3’ group
753 which had lower membership than expected (in bold).

754

755 **S2 Table. The average age for each epitope group.** The average age for the 138 specimens for
756 which there was age data was 35. The ‘None’ group had an average age of 50 which was notably
757 higher than the average age of 35 (in bold). Additionally, the ‘1+2+3’ group had a lower average
758 age of 17 (in bold). This discrepancy suggests that older people targeted fewer *Rhinovirus A*
759 epitopes.

760

761 **Table S3. Eight HSV2-specific epitopes were also in the HSV1 proteome.**

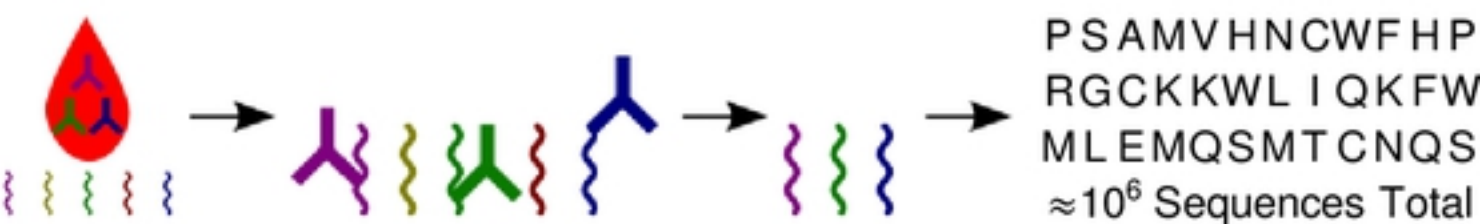
762

763 **Code S1. KTOPE software, written in Python 3.6.**

764

765 **Text S1. KTOPE usage guide.**

766

A**B**

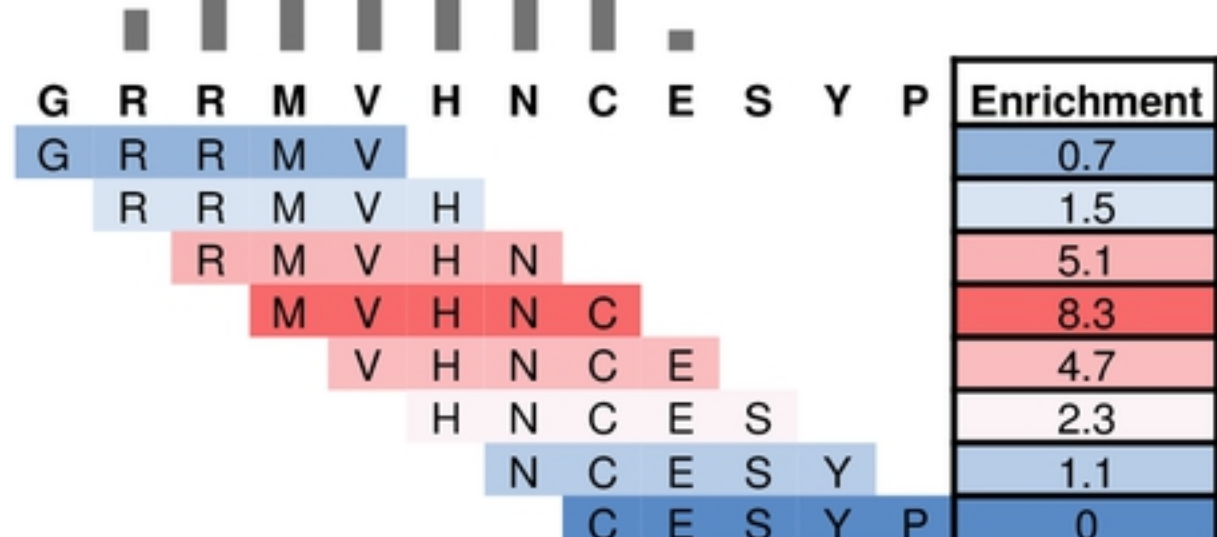
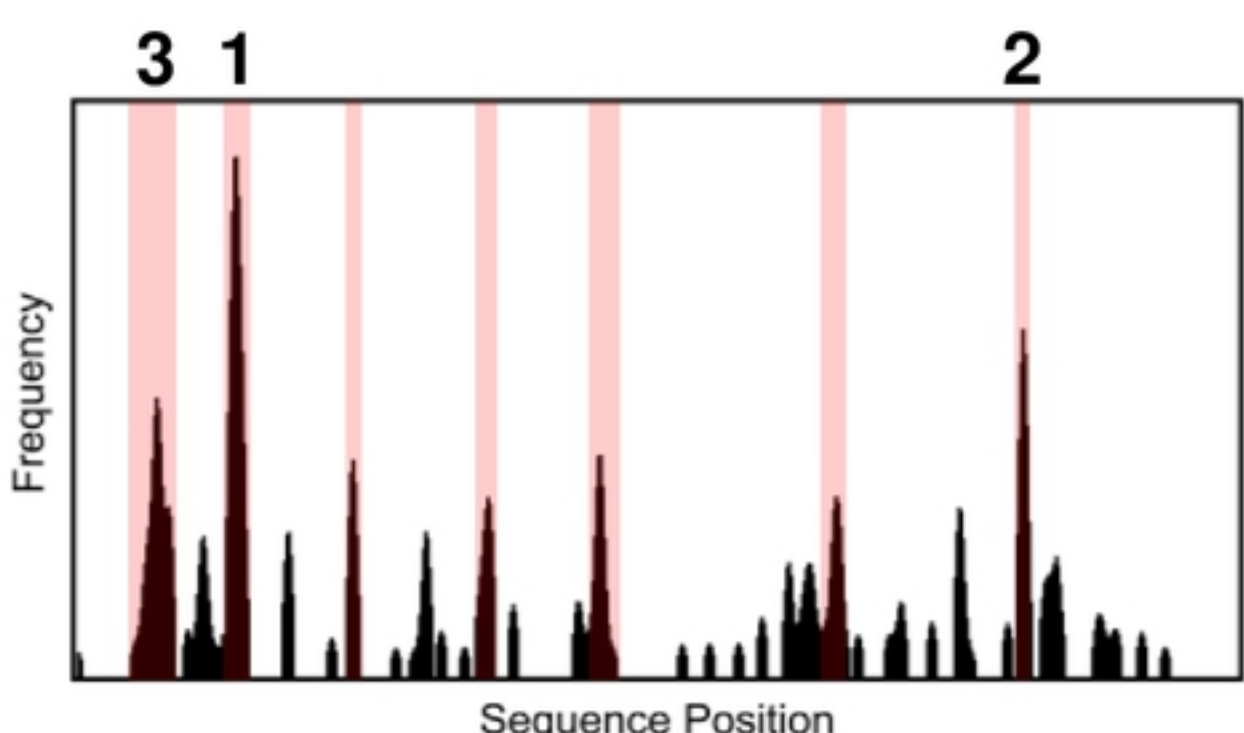
	K-mer	Enrichment
PSAM MVHNC WFHP	AAAAAA	1.1
GNPKLNGSATCP	CAAAAA	0.7
KSQ KNWNK IDVN	⋮	⋮
MEKAYMNLMHAP	KNWNK	4.3
RGCKKWL IQKFW	MLEMQ	1.4
ERSHTLKFITT I	MVHNC	15.3
MLEMQ SMTCNQS	⋮	⋮
EVLGKYKTQVYM	YYYYYY	1.0
CKVCARM MVHNC		

C

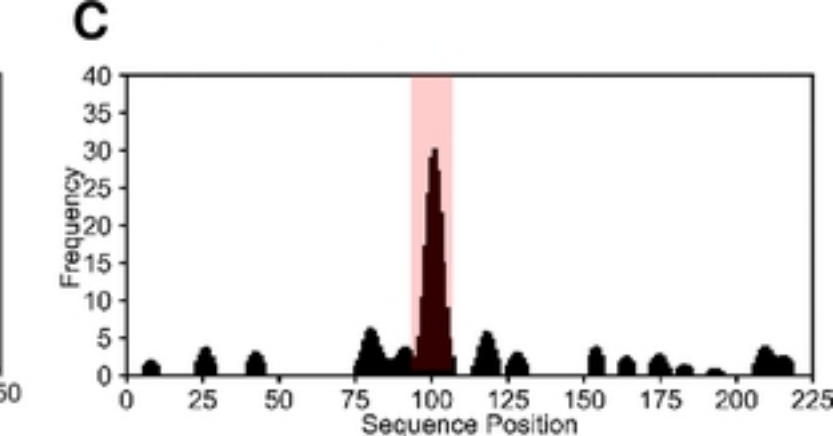
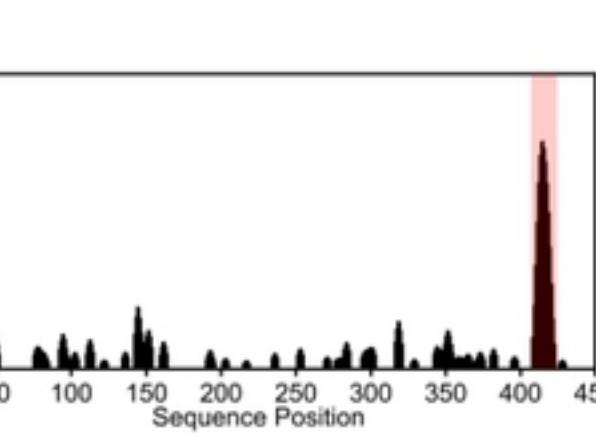
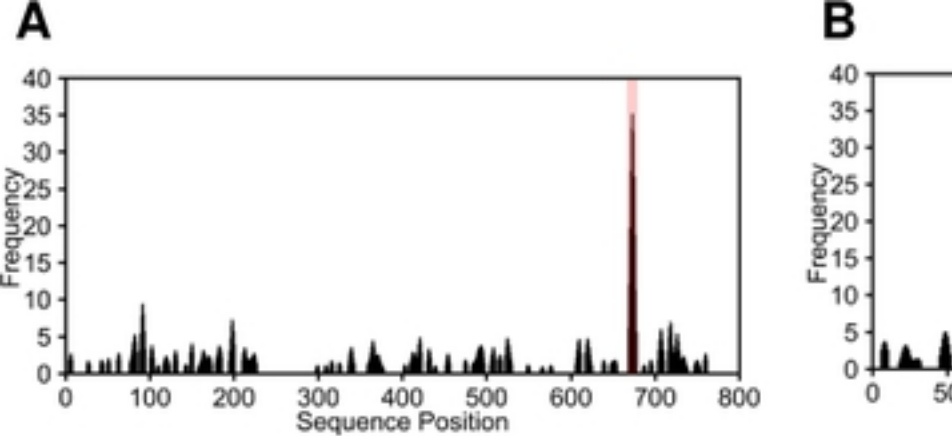
bioRxiv preprint doi: <https://doi.org/10.1101/641787>; this version posted May 17, 2019. The copyright holder for this preprint (which was not certified by peer review) is the author/funder, who has granted bioRxiv a license to display the preprint in perpetuity. It is made available under aCC-BY 4.0 International license.

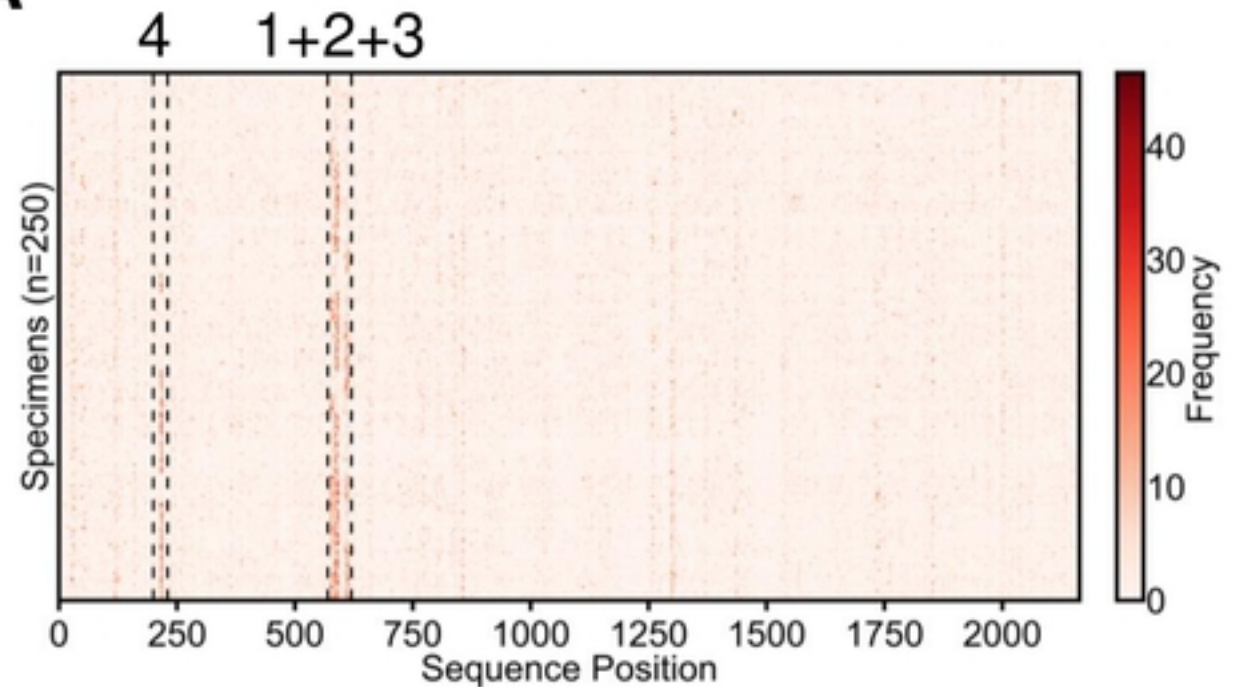
Protein Sequence:

...SGDSCAIVLHLFQTHEWCWNVIIPWIIKYREGKYKCNQPQYPD
DQDELPSRENPRFYNTSWTCHR**GRRMVHNCESY**SEGASFL...

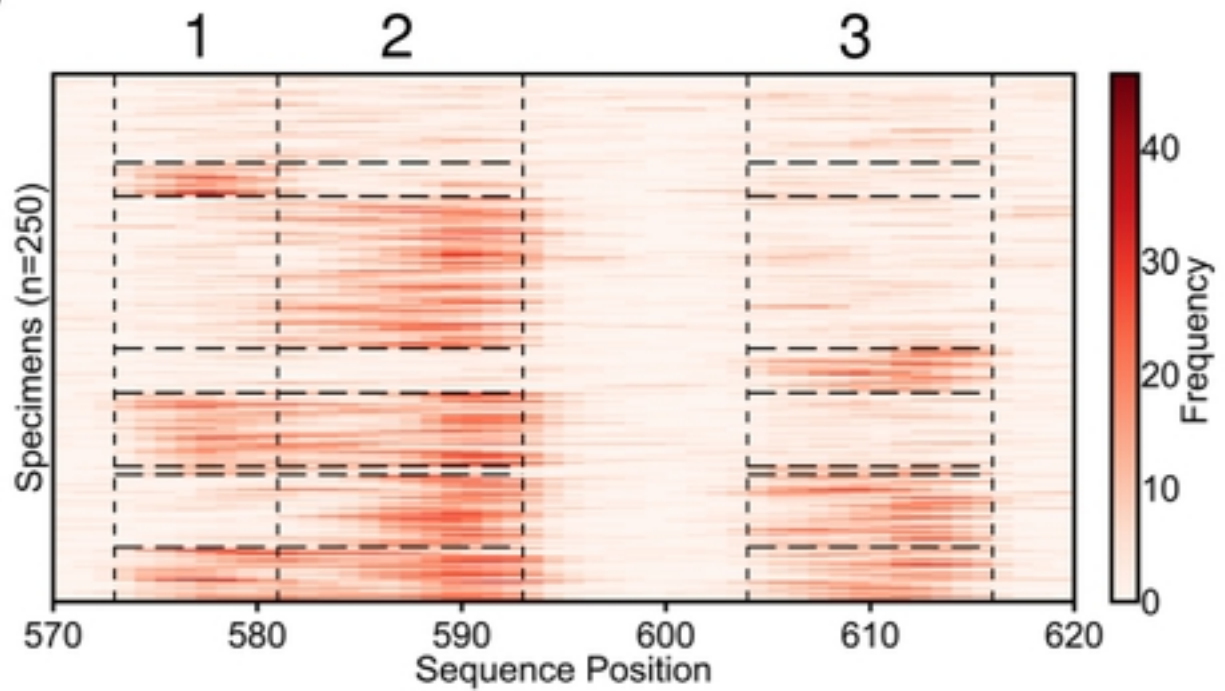
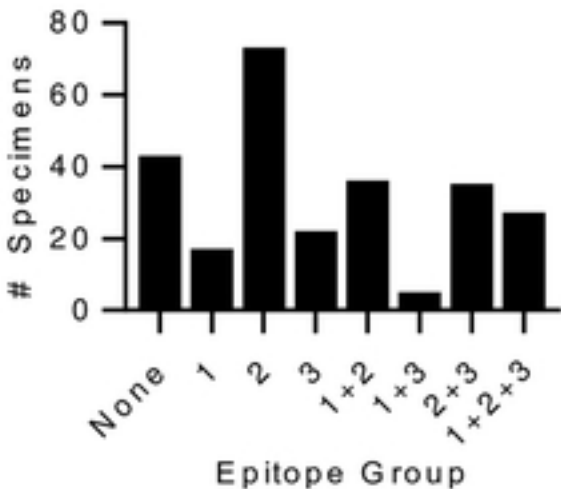
**D**

	Epitope	AUC Score	Percentile
1	PKEMPLESAEK	137	99%
2	RRMVHNCE	73	95%
3	AALNVNSKILDGTLG ENSSFTAVVLGGDA GMGDKATVE EVNRWWLHLP AYLCQFISHRYIELY	55 49 40 38 30	89% 64% 55% 40% 33%

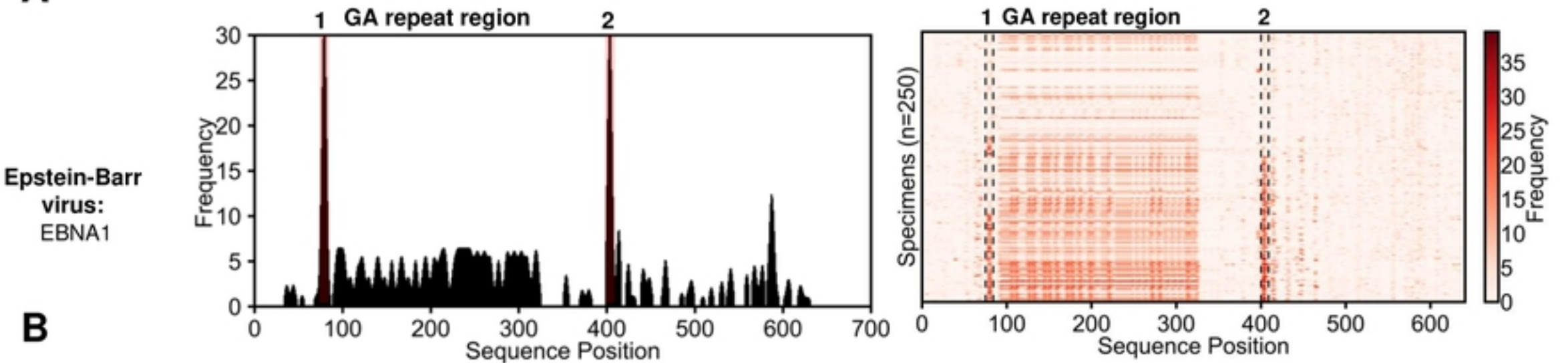


A**B**

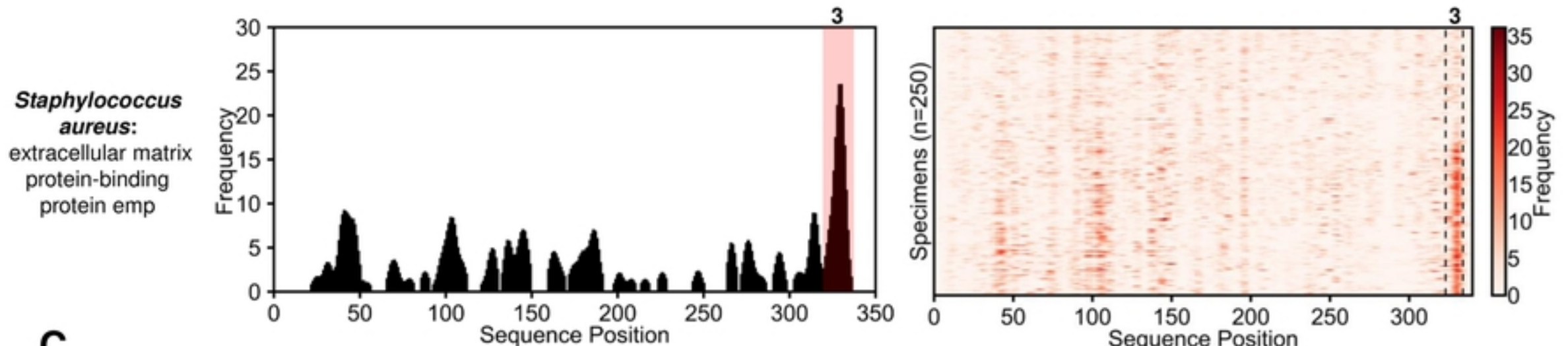
Epitope #	% Population Binds
1	32%
2	67%
3	34%
4	41%
Any of the 4	87%

C**D**

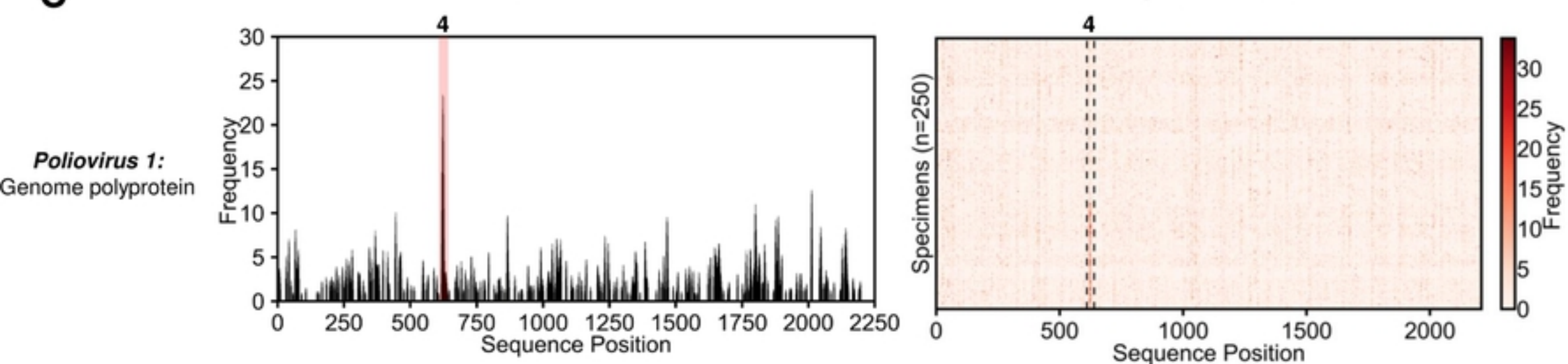
A



B

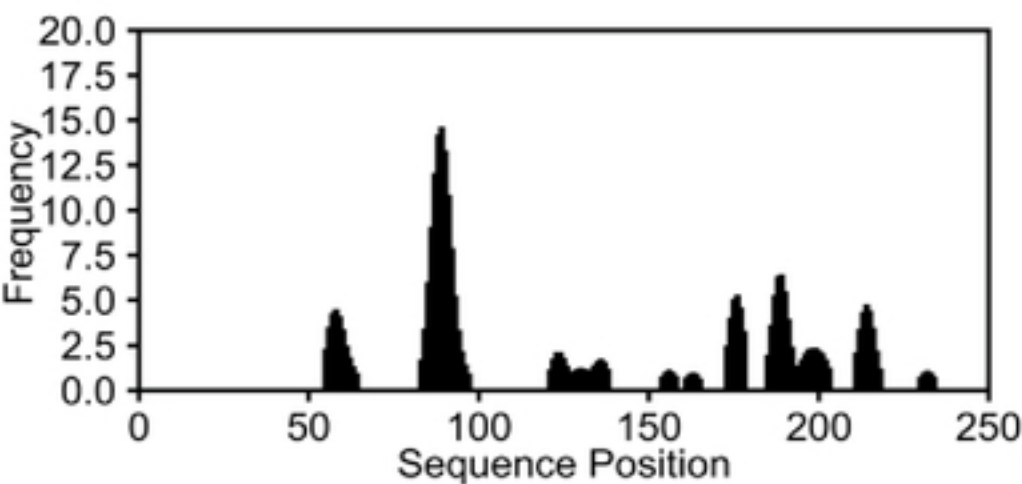
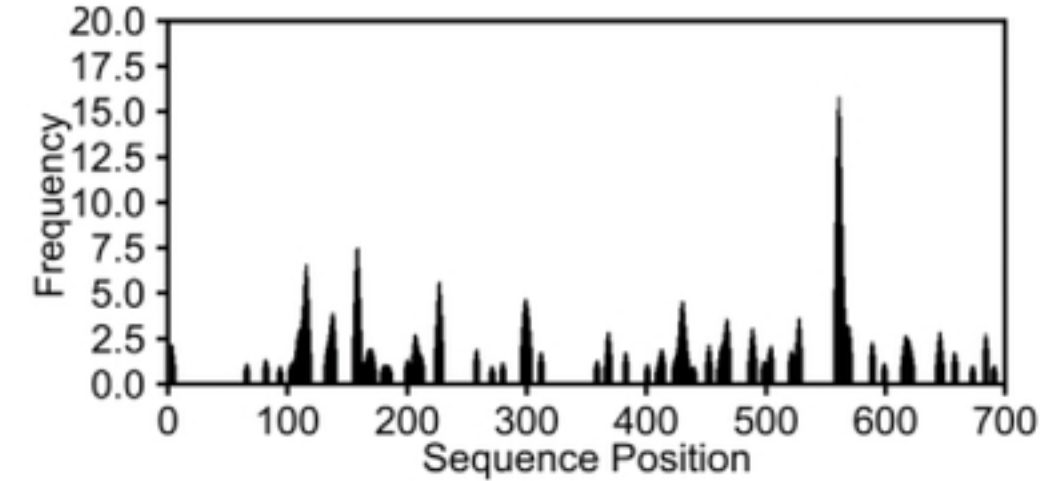
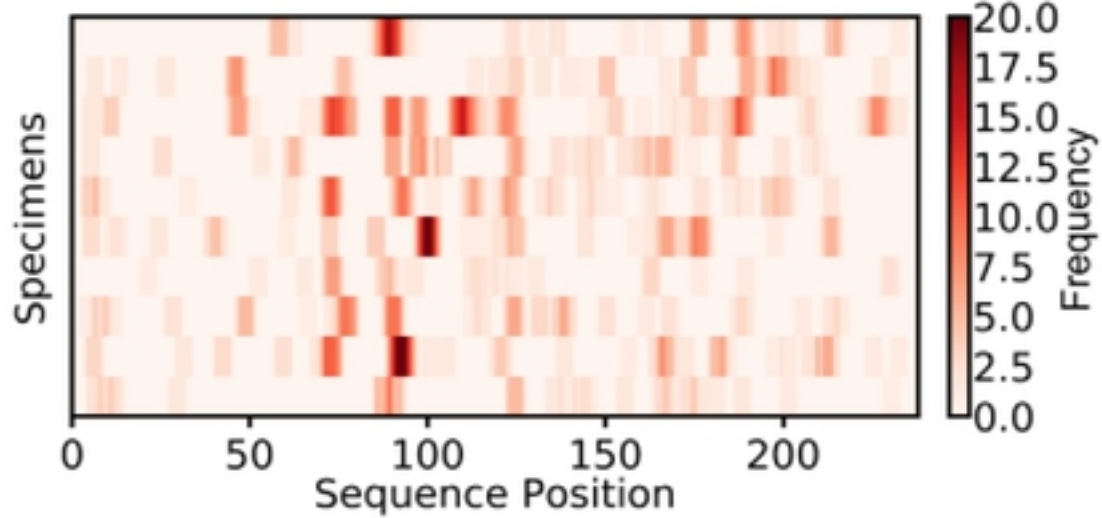


C



D

Peak #	Literature	K-TOPE	Prevalence	P-Value	Reference
1	KRPSCIGCK	RPSCIGCKG	0.40	0.0056*	[6]
2	RRPFF	PGRRPFFHP	0.52	0.0031	[33]
3	VPEFKGSLP	PTHYVPEFKGS	0.57	0.019	[40]
4	PALTAVETGATNPL	EIPALTAVETG	0.39	0.003	[35]

A**B****C****D**